Received: 14 January 2019 | Accepted: 28 January 2019

DOI: 10.1002/asna.201913579

ORIGINAL ARTICLE

Astronomische Nachrichten

Hyperonic neutron star matter in light of GW170817

W. M. Spinella[1,*] | **F. Weber**[2,3]

[1]Department of Sciences, Wentworth Institute of Technology, Boston Massachusetts
[2]Department of Physics, San Diego State University, San Diego California
[3]Center for Astrophysics and Space Sciences, University of California San Diego, California

***Correspondence**
W. M. Spinella, Department of Sciences, Wentworth Institute of Technology, Boston MA.
Email: spinellaw@wit.edu

Funding Information
National Science Foundation (USA), PHY-1714068.

Since 2013, the mass of pulsar PSR J0348 + 0432 ($M = 2.01 M_\odot$) has provided a tight constraint on neutron star (NS) equation of state. However, a number of different analyses of the recently detected binary neutron star (BNS) merger (GW170817) point to a maximum NS mass around $2.16 M_\odot$. In addition, a recent study determined the mass of the millisecond pulsar PSR J2215 + 5135 to be $2.27^{+0.17}_{-0.15} M_\odot$. In this work, we investigate the presence of hyperons in NS matter in light of these new mass measurements using equations of state calculated in the relativistic mean-field approximation. Particular attention is paid to the use of the available empirical data from the study of hypernuclei and that of the SU(3) symmetry relations in fixing the meson-hyperon coupling constants. We find that hyperonic equations of state with reasonable choices for the meson-hyperon coupling constants can satisfy these new mass constraints, with hyperons potentially accounting for more than 10% of the baryons in the core of a NS.

KEYWORDS
equation of state – gravitational waves – stars: neutron

1 | INTRODUCTION

Published mass measurements of PSR J1614-2230 in 2010 and PSR J0348 + 0432 in 2013 indicate that neutron stars (NSs) can have masses as large as twice the mass of our sun. Including hyperons in the modeled composition of NS matter increases the baryonic degrees of freedom softening the NS equation of state (EoS), the degree of which depends on the choice of meson-hyperon coupling constants in relativistic mean-field (RMF) models. This softening often results in a calculated maximum NS mass that is inconsistent with the aforementioned observations, giving rise to the so-called "hyperon puzzle." Common resolutions of the hyperon puzzle involve stiffening the EoS by introducing repulsive hyperon-nucleon and hyperon-hyperon interactions and adjusting the meson-hyperon coupling constants in various EoS models. However, analyses of the recent multimessenger observation of a binary neutron star (BNS) merger suggest a maximum NS mass significantly higher than two solar masses, as does the recently published measurement of the mass of PSR J2215 + 5135, reinvigorating the hyperon puzzle. Therefore, we seek to determine whether or not a reasonably constrained hyperonic NS matter EoS can produce a maximum mass consistent with these new constraints.

In this work, we compute the EoS of NS matter including the full baryon octet, using a RMF model consistent with constraints on the properties of the isospin-symmetric nuclear matter (SNM) EoS including the nuclear incompressibility and the isospin asymmetry energy and slope. EoS stiffening due to the inclusion of hyperon-hyperon interactions, mediated via strange-scalar (σ^*) and strange-vector (ϕ) mesons, is examined by calculating the NS properties for different combinations of mesons. Scalar meson-hyperon coupling constants are fit to empirical data on hypernuclei where available, while the vector meson-hyperon couplings are fixed by the SU(3) symmetry. By varying SU(3) coupling parameters, we traverse the entire vector meson-hyperon coupling space and calculate NS properties including the maximum mass, strangeness fraction, and hyperon fraction. We determine the couplings that are consistent with the mass constraints provided by PSR J0348 + 0432 and analyses of the detected

Abbreviations: BNS, binary neutron star; EoS, equation of state; NS, neutron star; RMF, relativistic mean-field; SNM, symmetric nuclear matter.

gravitational waves (GW170817) and gamma-ray burst (GRB 170817A) produced by the observed BNS merger.

This work is organized as follows. In Section 2, we introduce the RMF model and parameterization of the EoS, as well as the methods used for determining the meson-hyperon coupling constants. In Section 3, we discuss additional constraints on the EoS provided by analyses of GW170817 and GRB 170817A. Our results, including calculations of the NS properties for the vector meson-hyperon coupling space, are presented in Section 4. Finally, we provide a summary of this work in Section 5.

2 | EQUATION OF STATE

In this work, we calculate EoSs of cold, nonrotating NSs using the nonlinear RMF approximation, modeling baryon-baryon interactions in terms of scalar (σ, σ^*), vector (ω, ϕ), and isovector (ρ) meson fields, represented by the following Lagrangian,

$$\begin{aligned}\mathcal{L} = &\sum_{\mathrm{B}} \overline{\psi}_{\mathrm{B}}[\gamma_\mu \left(i\partial^\mu - g_{\omega\mathrm{B}}\omega^\mu - g_{\phi\mathrm{B}}\phi^\mu - \frac{1}{2}g_{\rho\mathrm{B}}\boldsymbol{\tau}\cdot\boldsymbol{\rho}^\mu \right) \\ &- (m_{\mathrm{B}} - g_{\sigma\mathrm{B}}\sigma - g_{\sigma^*\mathrm{B}}\sigma^*)]\psi_{\mathrm{B}} \\ &+ \frac{1}{2}(\partial_\mu\sigma\partial^\mu\sigma - m_\sigma^2\sigma^2) \\ &- \frac{1}{3}b_\sigma m_n(g_{\sigma N}\sigma)^3 - \frac{1}{4}c_\sigma(g_{\sigma N}\sigma)^4 \\ &- \frac{1}{4}\omega_{\mu\nu}\omega^{\mu\nu} + \frac{1}{2}m_\omega^2\omega_\mu\omega^\mu \\ &- \frac{1}{4}\boldsymbol{\rho}_{\mu\nu}\cdot\boldsymbol{\rho}^{\mu\nu} + \frac{1}{2}m_\rho^2\boldsymbol{\rho}_\mu\cdot\boldsymbol{\rho}^\mu \\ &- \frac{1}{4}\phi^{\mu\nu}\phi_{\mu\nu} + \frac{1}{2}m_\phi^2\phi_\mu\phi^\mu \\ &+ \frac{1}{2}(\partial_\mu\sigma^*\partial^\mu\sigma^* - m_{\sigma^*}^2\sigma^{*2}) \\ &+ \sum_\lambda \overline{\psi}_\lambda(i\gamma_\mu\partial^\mu - m_\lambda)\psi_\lambda. \end{aligned} \tag{1}$$

The EoS is parameterized to reproduce the following properties of SNM at a saturation density of $n_0 = .150$ fm^{-3}: the energy per nucleon $E_0/N = -16.0$ MeV, nuclear incompressibility $K_0 = 250.0$ MeV, effective nucleon mass $m^*/m_N = 0.70$, isospin asymmetry energy $S_0 = 30.3$ MeV, and the slope of the asymmetry energy $L_0 = 46.5$ MeV. The parameterization is specifically tailored for consistency with a number of simultaneous constraints on the asymmetry energy (S_0) and the slope of the asymmetry energy (L_0) at n_0 as shown in Figure 1. To satisfy the constraints on L_0, the isovector-vector meson-baryon coupling constants are taken to be density-dependent with a functional density-dependence given by (Drago et al. 2014; Typel & Wolter 1999)

$$g_{\rho\mathrm{B}}(n) = g_{\rho\mathrm{B}}(n_0)\exp[-a_\rho(n/n_0 - 1)], \tag{2}$$

with the parameter a_ρ fit to L_0 at n_0.

The EoS of SNM and mass-radius relation for the purely nucleonic EoS ($npe\mu$) are given in Figure 2. The low-density

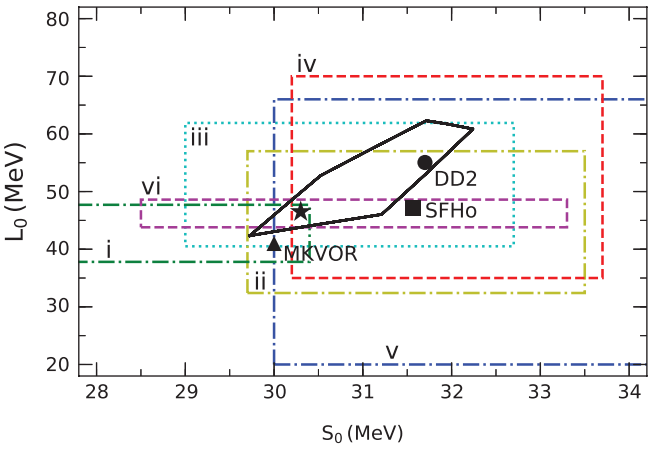

FIGURE 1 Symmetry energy and slope of the symmetric nuclear matter (SNM) parameterization at saturation density with the following constraints from the literature: (i) Hagen et al. (2015), (ii) Hebeler et al. (2013), (iii) Lattimer & Steiner (2014), (iv) Danielewicz & Lee (2014), (v) Roca-Maza et al. (2015), and (vi) Birkhan et al. (2017). The irregular black outline represents the accepted region determined from various experimental and theoretical constraints compiled in Figure 9 of Tews et al. (2017). The star marker indicates the values for the parameterization used in this work

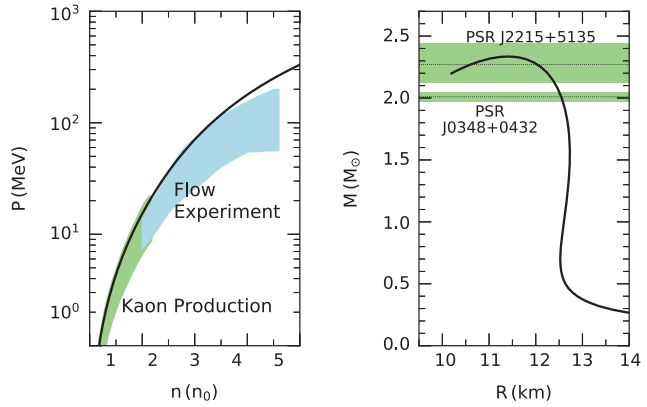

FIGURE 2 Equation of state (EoS) of symmetric nuclear matter (SNM) (left panel) and mass-radius relation for a purely nucleonic EoS (right panel), both including constraints discussed in the text

EoS is sufficiently soft to satisfy the constraint from kaon production and produce a relatively small canonical radius, while the high-density EoS is too stiff to fully satisfy the elliptic flow constraint but produces a high maximum mass ($M_{\max} = 2.33M_\odot$) consistent with the masses of PSR J0348 + 0432 ($M = 2.01 \pm 0.04M_\odot$) and PSR J2215 + 5135 ($M = 2.27^{+0.17}_{-0.15}M_\odot$) (Antoniadis et al. 2013; Danielewicz et al. 2002; Fuchs 2006; Linares et al. 2018; Lynch et al. 2009). Note that outer and inner crust EoSs are appended to the low density EoS (Douchin & Haensel 2001; Haensel & Pichon 1994).

2.1 | Meson-hyperon coupling constants

Inclusion of the hyperonic degrees of freedom softens the neutron star EoS, and the corresponding reduction of the maximum mass is extremely sensitive to the choice of meson-hyperon coupling constants. It is, therefore,

essential that the coupling constants be fixed using empirical data wherever possible.

The scalar meson-hyperon coupling constants $g_{\sigma Y}$ and $g_{\sigma^* Y}$ can be fit to hyperon single-particle potentials and self-potentials derived from the available empirical data on hypernuclei, but first the vector meson-hyperon couplings $g_{\omega Y}$ and $g_{\phi Y}$ must be specified. In SU(3) symmetry, the vector couplings can be written in terms of three parameters: the mixing angle θ_V, the $F/(F+D)$ ratio α_V, and the octet-singlet coupling ratio z (Dover & Gal 1984). The most commonly used values for these parameters are $\theta_V = 35.26^\circ$, $\alpha_V = 1$, and $z = 1/\sqrt{6}$, corresponding to SU(6) symmetry. However, sophisticated baryon-baryon interaction models such as the Nijmegen extended-soft-core model (ESC08) predict much lower values of the coupling ratio z ($z_{\mathrm{ESC08}} \approx 0.195$) that lead to stiffer EoSs and much higher maximum masses than those constructed using SU(6) symmetry (Rijken et al. 2010). Rather than calculating a single EoS constructed from fixed values of α_V and z, we will instead calculate NS maximum masses, strangeness fractions, and hyperon fractions for the z parameter space with $\alpha_V = 1$, and for the entire α_V-z parameter space. Note that the ϕ meson couples to the nucleons if $z \neq 1/\sqrt{6}$, and as a result $g_{\omega N}$ must be recalculated to restore the saturation properties of the RMF parameterization.

With the vector meson-hyperon couplings specified, the scalar couplings are set to reproduce empirical hyperon single-particle potentials at saturation, $U_Y^{(N)}(n_0)$, using the following,

$$U_Y^{(N)}(n_0) = g_{\omega Y}\overline{\omega}_0 + g_{\phi Y}\overline{\phi}_0 - g_{\sigma Y}\overline{\sigma}_0. \tag{3}$$

In this work, we employ the following hyperon potentials: $U_\Lambda^{(N)}(n_0) = -28$ MeV, $U_\Sigma^{(N)}(n_0) = +30$ MeV, and $U_\Xi^{(N)}(n_0) = -14$ MeV. If the strange-scalar field σ^* is included, the strange-scalar meson-Λ coupling constant $g_{\sigma^*\Lambda}$ is set to reproduce a saturation self-potential of $U_\Lambda^{(\Lambda)}(n_0) = -1$ MeV in isospin-symmetric Λ-matter, a value close to that suggested by the Nagara event Ahn et al. (2013), using the following,

$$U_\Lambda^{(\Lambda)}(n_0) = g_{\omega\Lambda}\overline{\omega}_0 + g_{\phi\Lambda}\overline{\phi}_0 - g_{\sigma\Lambda}\overline{\sigma}_0 - g_{\sigma^*\Lambda}\overline{\sigma}^*_0. \tag{4}$$

The other strange-scalar meson-hyperon couplings are determined relative to that of the Λ as follows (Oertel et al. 2015),

$$U_\Xi^{(\Xi)}(n_0) = 2U_\Lambda^{(\Lambda)}(n_0/2), \tag{5}$$

$$g_{\sigma^*\Sigma} = g_{\sigma^*\Lambda}. \tag{6}$$

The isovector-vector meson-hyperon coupling constants $g_{\rho Y}$ are given as follows,

$$g_{\rho\Lambda} = 0, g_{\rho\Sigma} = g_{\rho\Xi} = g_{\rho N}, \tag{7}$$

with the differences in hyperon isospins accounted for by the isospin operator in the Lagrangian (see Equation (1)).

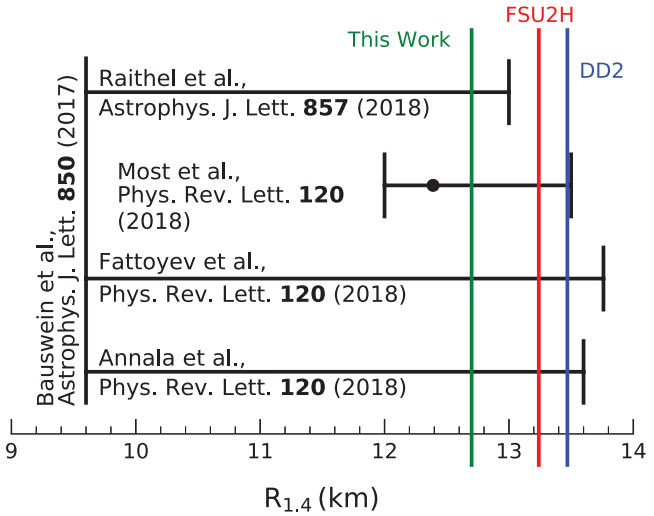

FIGURE 3 Constraints on the canonical neutron star (NS) radius derived using data from the recently observed binary neutron star (BNS) merger and gravitational wave signal GW170817 (Annala et al. 2018; Bauswein et al. 2017; Fattoyev et al. 2018; Most et al. 2018; Raithel et al. 2018)

3 | CONSTRAINTS FROM GW170817

Analyses of gravitational waves (GW170817) and a gamma-ray burst (GRB 170817A) emitted from the recent BNS merger have provided additional constraints on the NS EoS, with particularly tight constraints on hyperonic EoSs coming from estimates of the NS maximum mass (Abbott et al. 2017a, 2017b). A range of $2.15M_\odot \leq M_{\max} \leq 2.25M_\odot$ was determined from numerical relativity simulations and electromagnetic observations Shibata et al. 2017). Kilonova modeling suggests $2.01 \pm 0.04M_\odot \leq M_{\max} \leq 2.16^{+0.17}_{-0.15}M_\odot$, the lower limit taken to be the measured mass of PSR J0348+0432 (Rezzolla et al. 2018). Finally, analyses of the gamma-ray burst and kilonova ejecta provide an upper limit of $M_{\max} \leq 2.17M_\odot$ (Margalit & Metzger 2017). These maximum mass constraints are also relatively consistent with the measured mass of PSR J2215+5135. From these findings, and for the purposes of constraining the hyperonic EoSs calculated in this work, we determine a likely range for the maximum NS mass to be $2.01M_\odot \leq M_{\max} \leq 2.16M_\odot$ (Banik & Bandyopadhyay 2017).

Several constraints on the canonical radius have also been deduced from GW170817 and GRB 170817A and are presented in Figure 3. As shown, the EoS utilized in this work is consistent with these constraints with a canonical radius of 12.7 km. However, hyperons are not typically present in large enough quantities in a $1.4M_\odot$ NS to have an appreciable affect on the radius, so these constraints are not directly relevant to the hyperonic EoSs presented in the remainder of this work.

4 | RESULTS

A thorough investigation of hyperonic NS EoSs requires the calculation of NS properties for a large range of possible

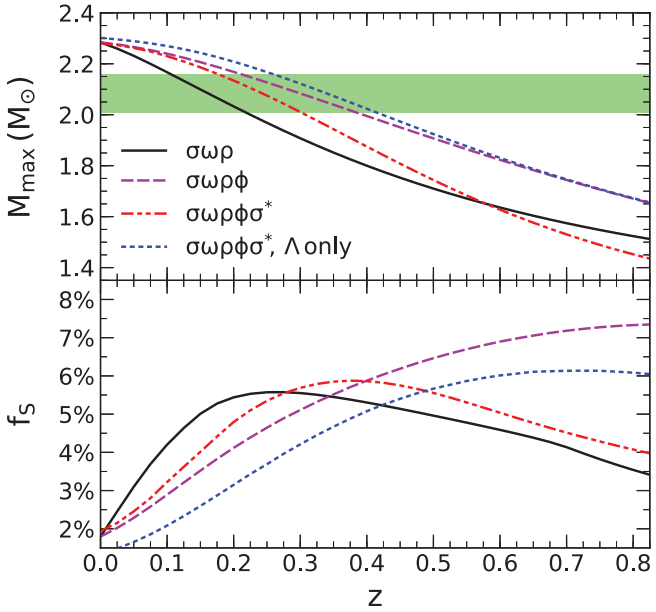

FIGURE 4 Maximum mass $M_{\max}$ (top panel) and strangeness fraction f_S (bottom panel) vs. z for equation of states (EoSs) with the inclusion of the indicated meson fields. The green highlighted region (top panel) extends from 2.01 to 2.16$M_\odot$, encapsulating mass constraints from PSR J0348 + 0432 and GW170817

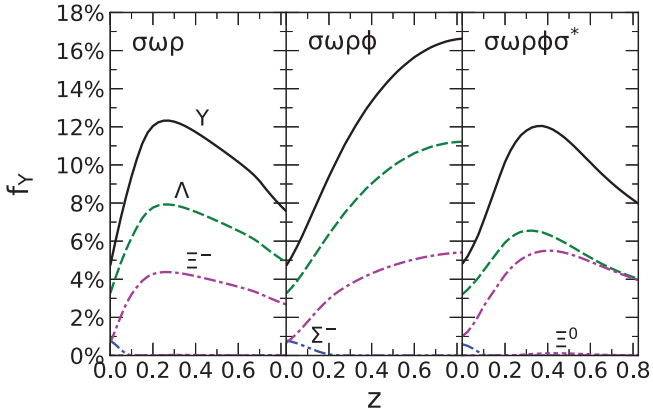

FIGURE 5 Maximum hyperon fractions f_Y vs. z for equation of states (EoSs) with the combinations of mesons shown in the different panels. The solid black line labeled Y represents the total hyperon fraction

TABLE 1 Required z, maximum strangeness fractions f_S, and maximum hyperon fractions f_Y for 2.01$M_\odot$ maximum mass neutron stars (NSs) extracted from the data in Figures 4 and 5

Model	z	f_S (%)	f_Y (%)
$\sigma\omega\rho$	.217	5.50	12.2
$\sigma\omega\rho\phi$	.382	5.76	13.0
$\sigma\omega\rho\phi\sigma^*$	.300	5.69	11.8
$\sigma\omega\rho\phi\sigma^*$, Λ only	.413	5.17	15.5

TABLE 2 The same as Table 1 but for 2.16$M_\odot$ maximum mass neutron stars (NSs)

Model	z	f_S (%)	f_Y (%)
$\sigma\omega\rho$	.105	4.30	9.58
$\sigma\omega\rho\phi$	.212	4.24	9.67
$\sigma\omega\rho\phi\sigma^*$	.177	4.46	9.58
$\sigma\omega\rho\phi\sigma^*$, Λ only	.257	3.76	11.2

meson-hyperon coupling constants. In this section, we will discuss the NS properties calculated for a range of vector meson-hyperon coupling constants specified by varying the α_V and z SU(3) coupling parameters, with the scalar meson-hyperon couplings fit to the hyperon saturation potentials as discussed in Section 2.1. To examine the affect of including hyperon-hyperon interactions, we will compute the NS properties for EoS models that include the σ, ω, and ρ mesons ($\sigma\omega\rho$), the ϕ meson ($\sigma\omega\rho\phi$), and the σ^* meson ($\sigma\omega\rho\phi\sigma^*$).

First we set $\alpha_V = 1$ and calculate the maximum mass ($M_{\max}$) and strangeness fractions (f_S) (Figure 4) as well as the maximum hyperon fractions (f_Y) (Figure 5) of NSs for all possible z. Decreasing z increases the values of the vector couplings $g_{\omega Y}$ and $|g_{\phi Y}|$, along with the maximum NS mass. The $\sigma\omega\rho\phi$ model produces a stiff EoS with maximum masses up to ~0.2$M_\odot$ greater than that of the $\sigma\omega\rho$ and $\sigma\omega\rho\phi\sigma^*$ models. However, if one considers the possibility that Σ and more importantly Ξ hyperons do not appear in NS matter, then the maximum mass of the $\sigma\omega\rho\phi\sigma^*$ model increases dramatically, the $\Xi-$ being responsible for considerable softening of the EoS. Total strangeness and hyperon fractions of the $\sigma\omega\rho\phi$ model increase monotonically with z, while those of the $\sigma\omega\rho\phi\sigma^*$ model reach maximums $f_S^{\max} \approx 6\%$ and $f_Y^{\max} \approx 12\%$ at $z \approx 0.37$ before decreasing with increasing z.

Results for the 2.01 and 2.16 $M_\odot$ mass constraint boundaries extracted from Figures 4 and 5 are summarized in Tables 1 and 2. Only by excluding the Σ and Ξ hyperons from the $\sigma\omega\rho\phi\sigma^*$ model can any of the calculated EoSs satisfy even the 2.01$M_\odot$ lower limit of the mass constraint, indicated by the bottom of the green-shaded region in Figure 4, if SU(6) symmetry ($z_{SU(6)} \approx .408$) is assumed, let alone the 2.16$M_\odot$ upper limit. If instead $z_{ESC08} \approx .195$ is chosen, the $\sigma\omega\rho\phi$ and $\sigma\omega\rho\phi\sigma^*$ models easily satisfy the 2.01$M_\odot$ constraint with maximum masses $M_{\max}(z_{ESC08}) \approx 2.17\,M_\odot$ and $M_{\max}(z_{ESC08}) \approx 2.14\,M_\odot$, respectively. However, the $\sigma\omega\rho\phi\sigma^*$ model requires z~.18 (just under $z_{ESC08c} \approx .182$) to satisfy the 2.16$M_\odot$ upper limit unless the Σ and Ξ hyperons are neglected, in which case z~.26 is sufficient.

Hyperon fractions in 2.16$M_\odot$ maximum mass NSs are substantial at nearly 10% when the entire baryon octet is included, with $f_\Lambda = 5.6\%$ and $f_{\Xi^-} = 3.9\%$ for the $\sigma\omega\rho\phi\sigma^*$ model. The fraction of Λs significantly exceeds that of the Ξ^- in the $\sigma\omega\rho$ and $\sigma\omega\rho\phi$ models, but the two are much more comparable when the σ^* meson is included as shown. As no experimental data from the study of double-hypernuclei yet exists to constrain the Ξ saturation self-potential, $g_{\sigma^*\Xi}$ was instead fixed theoretically using Equation (5). An overestimation of $g_{\sigma^*\Xi}$ will likewise overestimate f_{Ξ^-}, softening the hyperonic EoS. Therefore, it is possible that the $M_{\max}$ vs. z relation in

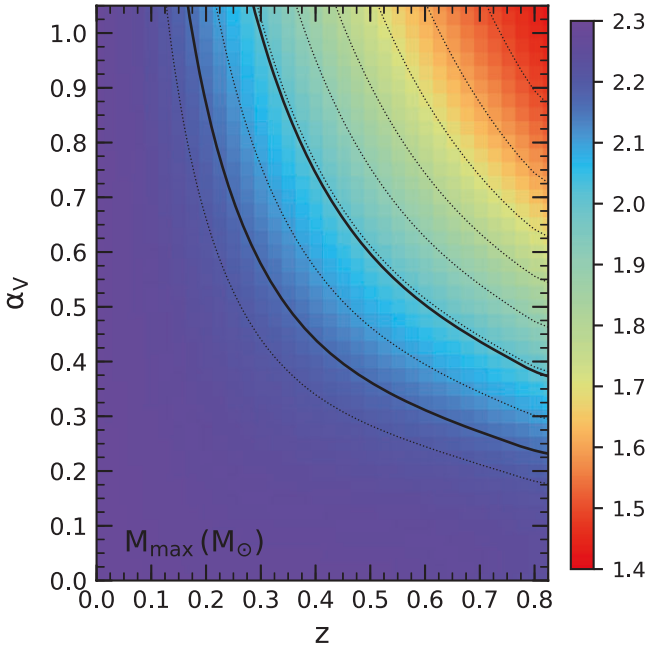

FIGURE 6 Maximum mass $M_{\max}(M_\odot)$ in the α_V vs. z SU(3) parameter space for equation of states (EoSs) calculated using the $\sigma\omega\rho\phi\sigma^*$ model. Dotted lines are maximum mass contours provided in $0.1M_\odot$ intervals, and solid lines represent the $2.01M_\odot$ and $2.16M_\odot$ contours bounding the region suggested by the mass of PSR J0348 + 0432 and analyses of GW170817

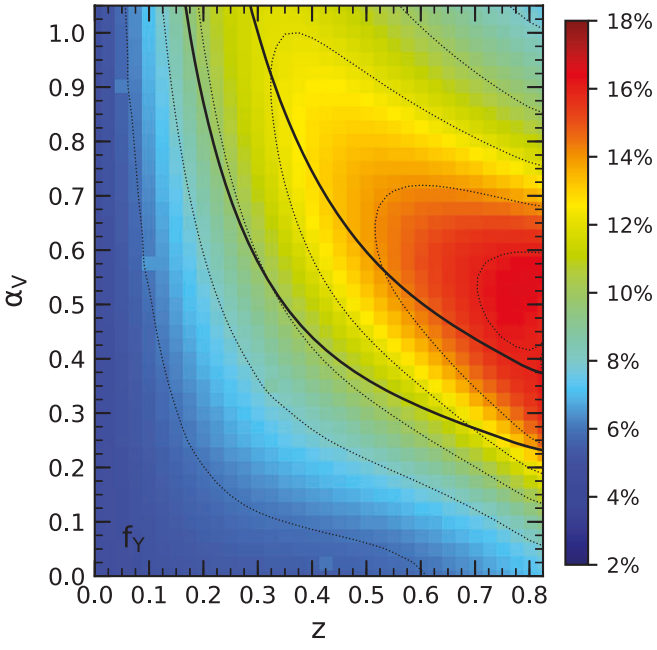

FIGURE 7 Hyperon fraction f_Y in the α_V vs. z SU(3) parameter space for EoSs calculated using the $\sigma\omega\rho\phi\sigma^*$ model. Dotted lines are hyperon fraction contours provided in 2% intervals. The solid lines represent the $2.01M_\odot$ and $2.16M_\odot$ contours bounding the region suggested by the mass of PSR J0348 + 0432 and analyses of GW170817 as shown in Figure 6

Figure 4 for the $\sigma\omega\rho\phi\sigma^*$ model may be closer to that displayed for the Λ hyperon alone, making the model more consistent with the stiff mass constraints deduced from GW170817. More experimental data from the study of hypernuclei and double-hypernuclei are sorely needed to sufficiently constrain the hyperon single-particle potentials and self-potentials.

Finally, we let both the α_V and z SU(3) parameters vary and calculate the maximum NS mass and hyperon fraction for the entire space using the $\sigma\omega\rho\phi\sigma^*$ model as shown in Figures 6 and 7. Neither α_V nor z is necessarily restricted by the $2.01 - 2.16M_\odot$ maximum mass constraint described by the bold contours in Figure 6. Increasing z beyond ~0.3 requires subsequent reduction of α_V below 1 to keep $M_{\max} > 2.01M_\odot$. A hyperon fraction hotspot is centered around $\alpha_V = .525$ and $z = .775$ with $f_Y^{\max} \approx 16.5\%$, while hyperon fractions consistent with the mass constraints range from 9.4 to 16%.

5 | SUMMARY

In this contribution, we introduced a new RMF parameterization, producing NS EoSs consistent with tight constraints on the isospin asymmetry energy and slope, and with constraints on the canonical NS radius deduced from analyses of the gravitational waves (GW170817) and gamma-ray burst (GRB 170817A) emitted by the recent BNS merger. This particular parameterization is of great utility in the study of hyperonization, as it is relatively straightforward to recover the intended saturation properties of SNM when choosing vector meson-hyperon coupling constants that are inconsistent with SU(6) symmetry ($z \neq 1/\sqrt{6}$).

We calculated the maximum mass, strangeness fraction, and hyperon fraction of NSs for hyperonic EoSs, exploring the full range of possible vector meson-hyperon coupling constants consistent with SU(3) symmetry. Maximum masses were compared to constraints deduced from analyses of GW170817 and GRB 170817A that suggest the maximum NS mass falls in the following range: $2.01M_\odot \lesssim M_{\max} \lesssim 2.16M_\odot$. Taking the SU(3) parameter $\alpha_V = 1$, we find this maximum mass range suggests $.18 \lesssim z \lesssim .30$ when considering the full baryon octet and including both the ϕ and σ^* mesons. However, if only the Λ hyperon is considered, we find that $.26 \lesssim z \lesssim .41$, highlighting the importance of acquiring additional empirical data with which to constrain the saturation single-particle potential and self-potential of the Ξ hyperon. Finally, the strangeness and hyperon fractions found for the $\sigma\omega\rho\phi\sigma^*$ model and the given maximum mass range are $4.5\% \lesssim f_S \lesssim 5.7\%$ and $9.6\% \lesssim f_Y \lesssim 12\%$, respectively.

ACKNOWLEDGMENTS

We thank D. Blaschke for his valuable comments regarding this manuscript. This research was supported by the National Science Foundation (USA), grant number PHY-1714068.

REFERENCES

Abbott, B. P., Abbott, R., Abbott, T. D. et al. 2017a, *Phys. Rev. Lett.*, *119*, 161101.
Abbott, B. P., Abbott, R., Abbott, T. D. et al. 2017b, *Astrophys. J. Lett.*, *848*, L12.
Ahn, J. K., Akikawa, H., Aoki, S. et al. 2013, *Phys. Rev. C*, *88*, 014003.

Annala, E., Gorda, T., Kurkela, A., & Vuorinen, A. 2018, *Phys. Rev. Lett.*, *120*, 172703.
Antoniadis, J., Freire, P. C. C., Wex, N. et al. 2013, *Science*, *340*, 6131.
Banik, S., & Bandyopadhyay, D. 2017, Dense Matter in Neutron Star: Lessons from GW170817. *arXiv e-prints*, 1712.09760, Provided by the SAO/NASA Astrophysics Data System, http://adsabs.harvard.edu/abs/2017arXiv171209760B.
Bauswein, A., Just, O., Janka, H.-T., & Stergioulas, A. 2017, *Astrophys. J. Lett.*, *850*, L34.
Birkhan, J., Miorelli, M., Bacca, S., et al. 2017, *Phys. Rev. Lett.*, *118*, 252501.
Danielewicz, P., & Lee, J. 2014, *Nucl. Phys. A*, *922*, 1.
Danielewicz, P., Lacey, R., & Lynch, W. G. 2002, *Science*, *298*, 1592.
Douchin, F., & Haensel, P. 2001, *Astron. Astrophys.*, *380*, 151.
Dover, C. B., & Gal, A. 1984, *Prog. Part. Nucl. Phys.*, *12*, 171.
Drago, A., Lavagno, A., Pagliara, G., & Pigato, D. 2014, *Phys. Rev. C*, *90*, 065809.
Fattoyev, F.-J., Piekarewicz, J., & Horowitz, C. J. 2018, *Phys. Rev. Lett.*, *120*, 172702.
Fuchs, C. 2006, *Prog. Part. Nucl. Phys.*, *56*, 1.
Haensel, P., & Pichon, B. 1994, *Astron. Astrophys.*, *283*, 313.
Hagen, G., Ekstrom, A., Forssen, C. et al. 2015, *Nat. Phys.*, *12*, 186.
Hebeler, K., Lattimer, J. M., Pethick, C. J., & Schwenk, A. 2013, *Astrophys. J.*, *773*, 11.
Lattimer, J. M., & Steiner, A. W. 2014, *Eur. Phys. J. A*, *50*, 40.
Linares, M., Shahbaz, T., & Casares, J. 2018, *Astrophys. J.*, *859*, 54.
Lynch, W. G., Tsang, M. B., Zhang, Y., Danielewicz, P., Famiano, M., Li, Z., & Steiner, A. W. 2009, *Prog. Part. Nucl. Phys.*, *62*, 427.
Margalit, B., & Metzger, B. D. 2017, *Astrophys. J. Lett.*, *850*, L19.
Most, E. R., Weih, L. R., Rezzolla, L., & Schaffner-Bielich, J. 2018, *Phys. Rev. Lett.*, *120*, 261103.
Oertel, M., Providencia, C., Gulminelli, F., & Raduta, A. R. 2015, *J. Phys. G*, *42*, 075202.
Raithel, C. A., Ozel, F., & Psaltis, D. 2018, *Astrophys. J. Lett.*, *857*, L23.
Rezzolla, L., Most, E. R., & Weih, L. R. 2018, *Astrophys. J. Lett.*, *852*, L25.
Rijken, T. A., Nagels, M. M., & Yamamoto, Y. 2010, *Prog. Theor. Phys. Suppl.*, *185*, 14.
Roca-Maza, X., Vinas, X., Centelles, M., et al. 2015, *Phys. Rev. C*, *92*, 064304.
Shibata, M., Fujibayashi, S., Hotokezaka, K., Kiuchi, K., Kyutoku, K., Sekiguchi, Y., & Tanaka, M. 2017, *Phys. Rev. D*, *96*, 123012.
Tews, I., Lattimer, J. M., Ohnishi, A., & Kolomeitsev, E. E. 2017, *Astrophys. J.*, *848*, 105.
Typel, S., & Wolter, H. H. 1999, *Nucl. Phys. A*, *656*, 331.

How to cite this article: Spinella WM, Weber F. Hyperonic neutron star matter in light of GW170817. *Astron. Nachr.* 2019;340:145–150. https://doi.org/10.1002/asna.201913579